LANGMUIR Article
Cite This: Langmuir XXXX, XXX, XXX−XXX
pubs.acs.org/Langmuir

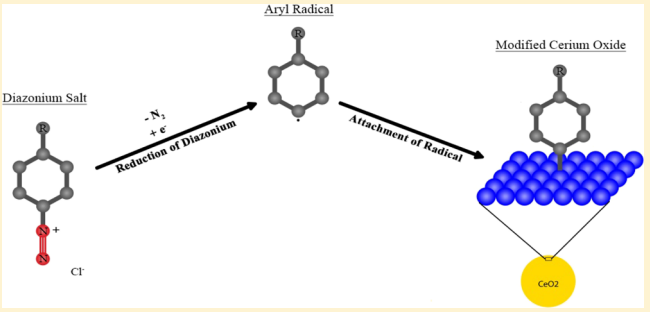
# Functionalization of Cerium Oxide Nanoparticles to Influence Hydrophobic Properties

Stephen Sanders and Teresa D. Golden*

Department of Chemistry, University of North Texas, 1155 Union Circle #305070, Denton, Texas 76203, United States

Supporting Information

**ABSTRACT:** Electroless functionalization of cerium oxide nanoparticles (NPs) based on the grafting of aryl groups from the reduction of diazonium salts is presented as a useful and facile method for enhancing the properties of the NPs. For this study, 4-methyl-, 4-ethyl-, and 4-*n*-butyl-benzene diazonium salts were used as model molecules to demonstrate the ability to change the hydrophobic properties of the cerium oxide ($CeO_2$) NPs. The grafting reaction was investigated under two reducing environments: the addition of a chemical reducing agent and the use of cerium oxide's native reducing property. Spectroscopic evidence for the successful attachment of aryl groups to the $CeO_2$ NPs was given by infrared and $^{13}C$ SS-NMR, which clearly detect characteristic aryl C−C peaks and the alkyl chains. X-ray diffraction results confirmed that the NPs underlying the crystal structure was unaffected by the grafting process. Thermal gravimetric analysis of the NPs suggested that this method enables the formation of multilayers at the surface, as well as an increase in the hydrophobic character. Hydrophobic properties of the resultant NPs further examined with a water contact angle test on pressed pellets revealed increase in hydrophobicity with increasing alkyl chain length. This research opens up new possibilities for controlling the surface chemical composition of $CeO_2$ NPs as well as other NPs using procedures operated in aqueous environments at room temperature.




## INTRODUCTION

Cerium oxide has been used in a wide variety of applications, including as a catalyst, as an electrolyte in solid-oxide fuel cells, in processes requiring a material of high refractive index, and as an insulating layer on silicon.[1−4] $CeO_2$ has also been used as a protective coating against corrosion on metals such as magnesium, aluminum, and steels.[5−7] Cerium oxide nanoparticles (NPs) can be produced by multiple processes including electrosynthesis, sonochemical, microwave heating, precipitation, pyrolysis, thermal decomposition, sol−gel, and mechanochemical methods.[8−16]

Many of cerium oxide's useful properties can be attributed to its ability to behave as a redox agent and change between the $Ce^{3+}$ and $Ce^{4+}$ redox states. Cerium oxide is well-known for its nonstoichiometry and oxygen vacancy formation.[2,17−19] Likely, the C-type cerium sesquioxide ($Ce_2O_3$) co-exists with fluorite cerium dioxide in nanosized cerium oxide, so that the nanosized cerium oxide should be $CeO_{2-x}$ instead of $CeO_2$. Metal atoms occupy the same positions in C-type structures as in fluorite structures, while the unit cell of C-type structures is twice the size of fluorite structures.[20,21] An increase in the lattice parameter with decreasing particle size has been shown and caused by the conversion of $Ce^{4+}$ to $Ce^{3+}$. This redox ability of nanosized cerium oxide is important for the function of cerium oxide as a catalyst. Some reactions in which $CeO_2$ has been used as a catalyst, such as the selective catalytic reduction of nitrogen oxides, can be prone to catalyst inhibition because of water contamination.[22,23] Because these catalyst reactions occur at the surface of the cerium oxide, surface functionalization is an important route to extend the range of potential applications.

The functionalization of surfaces by diazonium salt chemistry is a well-known phenomenon. The grafting proceeds via a reduction of the diazonium functional group, in which the C−N bond of the diazonium is cleaved via either a homolytic or heterolytic pathway, producing either an aryl radical or aryl cation, respectively.[24] The aryl radical or cation can then proceed to attach to the surface of the material being modified. The dediazonation reaction can be initiated in various ways, including electrochemically,[25,26] using a reducing substrate or reducing agents,[27] and photochemically.[28] Multiple types of surfaces can be modified using diazonium salt chemistry, including metals (such as copper, nickel, iron, gold, silver, platinum/iridium),[29−35] semiconductors,[36] and oxides (e.g., $TiO_2$, $MnO_2$).[37,38] Carbon nanotubes have also been modified through the use of diazonium salt chemistry.[39] Interest in using aryl diazonium salt chemistry to functionalize the surface of NPs (Si, $Fe_3O_4$, and gold) has also been expressed

Received: January 21, 2019
Revised: March 24, 2019
Published: April 10, 2019

Downloaded via UNIV OF NORTH TEXAS on April 22, 2019 at 13:18:36 (UTC).
See https://pubs.acs.org/sharingguidelines for options on how to legitimately share published articles.


© XXXX American Chemical Society

DOI: 10.1021/acs.langmuir.9b00201
Langmuir XXXX, XXX, XXX−XXX

recently.[40−42] The desired function of these NPs has ranged from increased stability in aqueous solutions to improved lithium storage capacity in battery applications, both of which illustrate the variety of properties that can be controlled or enhanced by diazonium-based grafting.

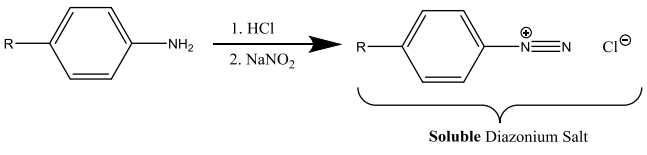
This work presents the electroless reduction of diazonium salts in aqueous solution as an easy means for the functionalization of cerium oxide NPs. Electroless grafting to cerium oxide NPs is a useful alternative to the electrochemical reduction of diazonium salts. Most grafting of diazonium salts to surfaces occurs through the connection of the surface to an electrochemical circuit while a potential is applied to reduce the diazonium group. Because the NPs are suspended in solution, and the electrochemical method is not viable, an electroless method is required. In this work, both the inherent redox capabilities of the $CeO_2$ NPs and the addition of a mild reducing agent (ascorbic acid) were used for the grafting of 4-methylbenzene, 4-ethylbenzene, and 4-*n*-butylbenzene groups to cerium oxide NPs. Ultrasonication was used to disperse NPs in the solvent, and ascorbic acid was used to produce aryl radicals by homolytic cleavage of the C−N bond. The reaction is performed in water, which lends to easier industrial use and also an environmentally friendly solvent.

The resulting NP materials were characterized by infrared (IR) spectroscopy, solid-state $^{13}C$ nuclear magnetic resonance (NMR), X-ray diffraction (XRD), thermal gravimetric analysis (TGA), and water contact angle tests. IR and NMR spectra confirmed grafting of the organic modifiers to the NP surface. XRD patterns obtained before and after grafting monitored any changes in the structure and morphology of the NPs. TGA determined the amount of grafted material on the surface of the NPs. Water contact angle tests verified changes in hydrophobicity among the resultant NPs. Because cerium oxide is normally slightly hydrophilic, this work focuses on increasing the physical property of hydrophobicity but could be extended to modify other chemical/physical properties of the cerium oxide.

## EXPERIMENTAL SECTION

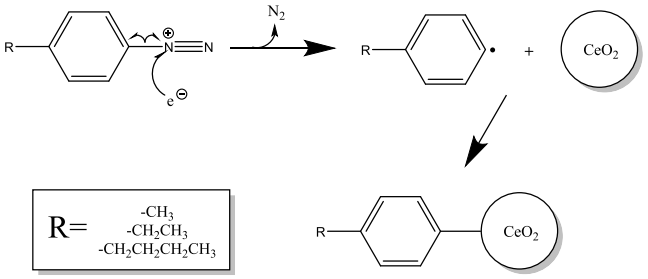
(**Caution**: Some diazonium salts such as chloride salts are unstable and can be explosive. Use proper preparation and safety protocols.[43]) All diazonium salts were prepared from the corresponding anilines: *p*-toluidine, 4-ethylaniline, and 4-*n*-butylaniline (ACROS Organics). For grafting of the diazonium salts, the anilines were dissolved with 3 molar equivalents of hydrochloric acid (Fischer Scientific, ACS grade) and 1.1 molar equivalents of a concentrated sodium nitrite solution (Fischer Scientific, ACS grade) to produce a soluble chloride salt, in accordance with the established procedure.[44] The reaction is presented in Scheme 1. To characterize the diazonium salts by IR spectroscopy, insoluble diazonium salts were also prepared using tetrafluoroboric acid instead of hydrochloric acid, Supporting Information Scheme S1. (**Safety note**: Characterization studies of the diazonium salts are best performed using the tetrafluoroborate or tosylates diazonium salts, because the diazonium chloride salts can be unstable and pose explosive hazards).

**Scheme 1. Formation of Soluble Diazonium Salts for Use in Grafting Reactions**




Grafting of the diazonium salts onto the cerium oxide NPs was accomplished by adding dropwise a 0.1 M aqueous solution of the chloride diazonium salt to 20 g/L of cerium oxide NPs (Nanostructured & Amorphous Materials Inc., 99.95% Rare Earth Oxide, 20−30 nm approximate particle size), which were suspended in water by sonication. Previous studies have shown that the grafting of diazonium salts onto surfaces proceeds via a homolytic breaking of the C−N bond, forming an aryl radical and nitrogen gas.[24] The grafting procedure was performed by two different methods; one allows the natural reduction abilities of cerium oxide to form the bond, and the other uses a mild reducing agent, ascorbic acid. For ascorbic acid addition, 1 molar equivalent of ascorbic acid (Alfa Aesar, 99+ %, ACS grade) was added to the final solution to reduce the diazonium salt onto the NP. Reduction of the diazonium salt was accompanied by the release of nitrogen gas and an immediate color change in the NPs from yellow to brown. The grafting process is illustrated in Scheme 2.

**Scheme 2. Grafting of the Alkylbenzene Diazonium Salts to Cerium Oxide NPs**




After formation of the grafted NPs, the solutions were centrifuged at 6500 rpm for 1−2 h using a Thermo Scientific Biofuge Primo to collect the NPs. The NPs were then resuspended in a 50% ethanol solution to remove any ungrafted or loosely adsorbed organic species. Before characterization, the NPs were centrifuged and washed with the 50% ethanol solution at least 3 times or until the supernatant ran clear; then washed a final time with acetone. All NP samples were dried at 40 °C to help remove water.

A PerkinElmer spectrum one Fourier transform infrared (FT-IR) spectrophotometer with an attenuated total reflection attachment was used to analyze the composition of the diazonium salts, as well as the ungrafted and grafted NPs. Each sample was scanned 16 times at a wavenumber range of 4000−400 $cm^{-1}$. Solid-state NMR was performed using a Varian 500 to obtain the solid-state $^{13}C$ spectra of the samples. For NMR, each sample was run at a frequency of 125 MHz. The structure and phase composition of the bare $CeO_2$ NPs as well as the grafted samples were identified by XRD with a Siemens D500 diffractometer using Cu K$\alpha$ radiation ($\lambda$ = 1.5405 Å) in a standard Bragg−Brentano configuration. The X-ray tube was operated at 35 kV and 24 mA. Each sample was scanned from 20° to 75° (2$\theta$), with a step size 0.05° and a dwell time of 1.0 s. Thermal gravimetric analyses were performed on a TA Instruments Q50 TGA. For each sample, approximately 10 mg was loaded on a platinum dish, and heated from 50 to 700 °C at a rate of 15 °C/min. To compare the hydrophobicity of the resulting NPs, a pressed pellet of each NP sample was prepared using a 3 cm die set and a Carver Model C Laboratory Press at 20 000 psi. The contact angle of a water droplet was measured on the pressed pellet samples. The contact angle was measured by the static sessile drop method in which a camera records an image of the drop on the sample surface. Drops were dispensed by a 2 mL Ramé-Hart microsyringe graduated in 2 $\mu$L increments. The droplet size was 6 $\mu$L. Images of the droplets were recorded with an Infinity 2 CCD camera and Infinity Analyze 6.4 software. The angle between the liquid/solid interface and the liquid/vapor interface was measured by the Drop Shape Analysis ImageJ plugin. Contact angle values are reported as the average of measurements of three different positions.


DOI: 10.1021/acs.langmuir.9b00201
Langmuir XXXX, XXX, XXX−XXX

## RESULTS AND DISCUSSION

The procedure to graft alkylbenzene groups to cerium oxide NPs is shown in Schemes 1 and 2. Surface modification by the alkylphenyl groups was accomplished in two ways: reduction of the diazonium salts in solution by the cerium oxide NPs, and by adding ascorbic acid as a reducing agent. When the cerium oxide was allowed to act as the reducing agent, reaction times of up to 24 h were needed to complete the reduction of the diazonium salt. The choice to use ascorbic acid as a reducing agent in addition to the natural redox behavior of cerium oxide was made to verify whether speeding up the reaction would affect the efficiency of the grafting reaction. The reaction was completed in 1 h when ascorbic acid was used, and characterization (by IR, NMR, TGA, and water contact angle) of the resultant-modified NPs revealed no significant differences between the two different methods.

The FT-IR spectra of bare $CeO_2$ NPs and grafted samples are shown in Figure 1. Curve A is the spectrum of the bare

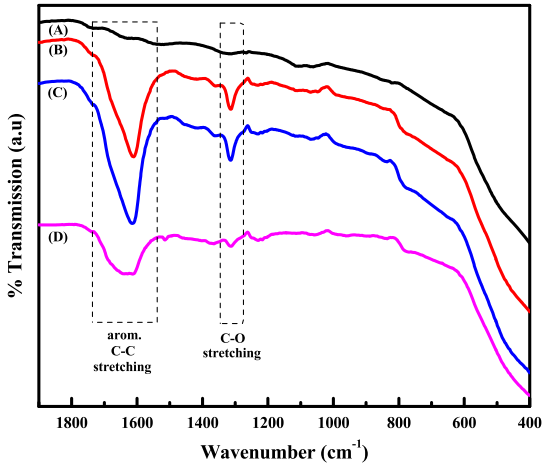



**Figure 1.** IR spectra of (A) ungrafted $CeO_2$ NPs and $CeO_2$ NPs grafted with (B) 4-methylbenzene diazonium chloride, (C) 4-ethylbenzene diazonium chloride, and (D) 4-*n*-butylbenzene diazonium chloride. The peak at 1617 $cm^{-1}$ indicates the presence of an aromatic ring (ring-breathing mode), and the peak at 1314 $cm^{-1}$ confirms the formation of a C−O bond between the diazonium and the NPs.

$CeO_2$ NPs and displays no peaks of interest in the 450−1900 $cm^{-1}$ range. All three of the grafted NP samples have similar peaks over this same range (curves B−D). The two peaks that appear for the grafted samples are at 1617 and 1314 $cm^{-1}$. The peak at 1617 $cm^{-1}$ can be attributed to the aromatic ring-breathing mode that was also observed at a similar wavenumber in the diazonium salt spectra (Supporting Information, Figure S1). The peak at 1314 $cm^{-1}$ is a result of the aryl radical produced from reduction of the diazonium salt forming a C−O bond to the oxygen present on the surface of the $CeO_2$. This C−O bond formation agrees with similar findings in the grafting of aryl diazonium salts to $MnO_2$ nanorods and $TiO_2$ electrodes.[37,38]

Furthermore, Figure 2 shows the absence of the band at 2300 $cm^{-1}$ (previously assigned to the N≡N stretching vibration) in the product spectra (Supporting Information, Figure S1), which indicates the loss of the diazonium group. These results strongly suggest that the grafting occurs by covalent attachment of the alkylphenyl moieties to the $CeO_2$ NP surface, with the loss of the diazonium group (see Scheme

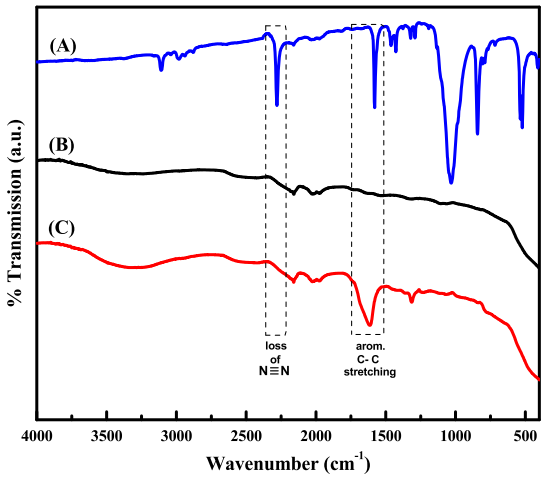



**Figure 2.** IR spectra of (A) 4-ethylbenzene diazonium salt, (B) ungrafted $CeO_2$ NPs, and (C) $CeO_2$ NPs grafted using 4-ethylbenzene diazonium chloride.

2). Intensity of the peaks in the product spectra did not change with the addition of ascorbic acid as compared to longer reaction times with no added reducing agent; thus, the grafting reaction was just as effective with the use of ascorbic acid. One other aspect of the IR spectra of the grafted NPs that is important to mention is the shift in aromatic C−C stretching from 1580 $cm^{-1}$ to a higher wavenumber at around 1617 $cm^{-1}$. This shift could be because of the change in the atom that the aromatic ring is bonded to form nitrogen in the diazonium to the more electronegative oxygen in the cerium oxide. This shift in the IR spectra has been demonstrated for other grafted NPs, such as $Fe_2O_3$, where grafting of the organic layers was used to make the $Fe_2O_3$ more water soluble.[38]

To further confirm the presence of alkylbenzene groups bonded to the $CeO_2$ NPs, solid-state $^{13}C$ NMR was performed on the NPs before and after the grafting reaction. Figure 3 presents the $^{13}C$ NMR spectra for (A) bare NPs and NPs grafted using (B) 4-methylbenzene, (C) 4-ethylbenzene, (D) 4-*n*-butylbenzene diazonium chloride. The spectra show the appearance of alkyl carbon signals between 0 and 50 ppm along with a signal around 130 ppm, which corresponds to the aromatic carbons. These results are further evidence of the successful grafting of the alkylphenyl groups onto the surface of the NPs.

Of special interest is that the alkyl carbon signal (0−50 ppm range) does not continue to increase linearly with the number of carbons in the alkyl chain. While the methyl carbon yields one signal and the ethyl carbons yield two, the butyl carbons yield only three signals where four might be expected. To investigate why this phenomenon occurs, a solution $^{13}C$ NMR spectrum was obtained using the aniline precursor, 4-*n*-butylaniline. NMR (Supporting Information, Figure S2) confirms that for the spectrum of 4-*n*-butylaniline, the signals for the two carbons closest to the aromatic ring are within 1 ppm of each other. Resolution of the solid-state NMR was insufficient to resolve these two peaks, and they appear as one in the corresponding solid-state spectrum.

XRD was conducted on the ungrafted and grafted $CeO_2$ NPs to determine whether the bond formation of the aryl radical to the NP was confined to the surface and if it had any effect on the underlying crystal structure. Figure 4 shows the XRD patterns of the NPs, and both grafted and ungrafted samples


DOI: 10.1021/acs.langmuir.9b00201
Langmuir XXXX, XXX, XXX−XXX

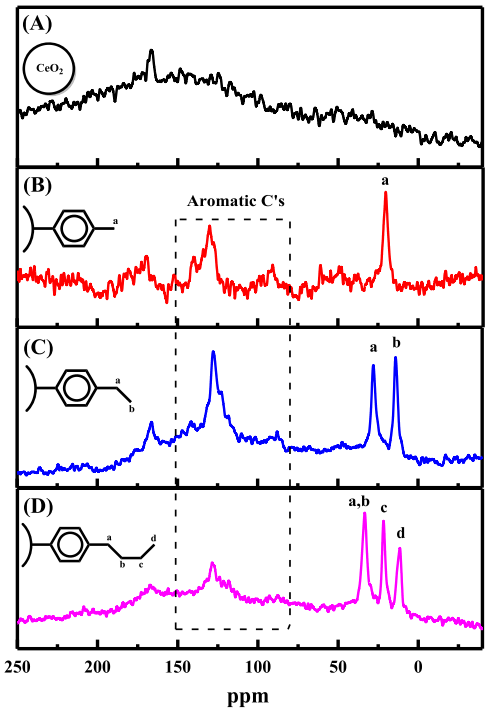



**Figure 3.** $^{13}C$ NMR spectra of (A) ungrafted $CeO_2$ NPs and $CeO_2$ NPs grafted with (B) 4-methylbenzene diazonium chloride, (C) 4-ethylbenzene diazonium chloride, and (D) 4-*n*-butylbenzene diazonium chloride. The $^{13}C$ NMR spectra show the appearance of methyl, ethyl, and *n*-butyl carbon peaks between 0 and 50 ppm as well as an aromatic carbon peak around 130 ppm.

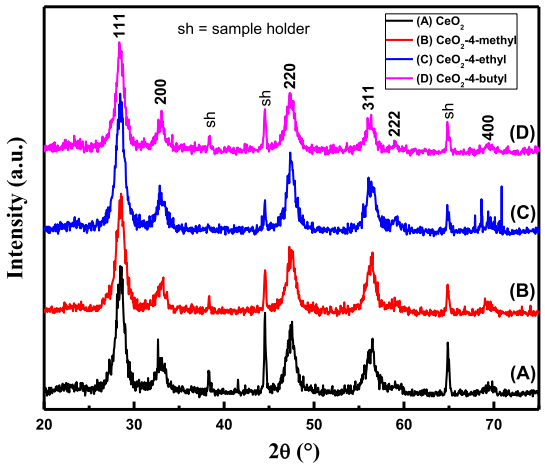



**Figure 4.** XRD patterns of the ungrafted (A) and grafted $CeO_2$ particles (B–D) displaying the characteristic peaks of the cubic fluorite structure. No observable changes were present in the grafted samples.

exhibit the characteristic peaks for the structure of $CeO_2$ (cubic fluorite structure, space group *Fm*3*m*) (JCPDS-00-034-0349). No new crystal phases are present after grafting, and the peak positions for each reflection are not shifted by the grafting process. This fact is important because it confirms that neither the reducing agent nor the organic group grafted to the surface affects the structure of the underlying NPs. Furthermore, according to the Scherrer equation, crystallite size is inversely proportional to the full-width-half-maximum (fwhm) of the peaks, meaning that a broader peak indicates a smaller crystallite size. From the XRD patterns of the NPs, the calculated particle size for all samples was between 20 and 25 nm, which is expected because the NPs obtained were advertized as ranging from 20 to 30 nm. The absence of a statistically significant change in the fwhm of the peaks in the XRD patterns when comparing before grafting to after grafting, indicates that the grafting process has no effect on the crystallite size of the NPs.

TGA was run on the NPs to determine how much organic material could be grafted effectively to the surface. Figure 5

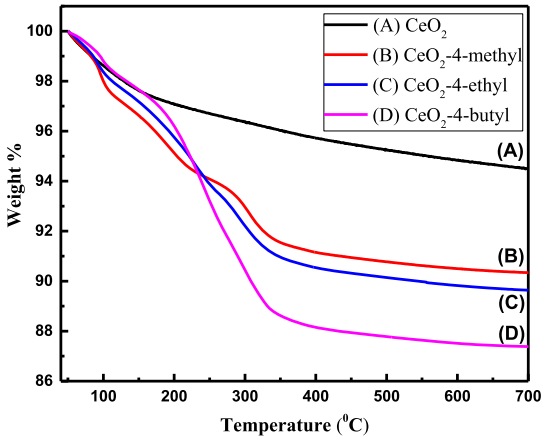



**Figure 5.** Weight loss curves for both ungrafted (A) and grafted NPs (B–D) shown as a percentage of initial weight.

confirms that loading of the organic material to the NPs fell consistently within the range of 8–10% by weight after accounting for water loss, regardless of the diazonium salt used. An interesting result was noted when the derivative of the weight loss was plotted against temperature. Figure 6 presents derivative weight loss plots for each of the ungrafted and grafted NP samples. They all show a peak indicating water loss around 100 °C.

However, for each of the grafted samples, there are additional two peaks showing weight loss of the organic species grafted to the NPs. This result suggests two different sites for grafting: a primary site directly on the NP surface; and secondary sites that start forming multilayers by grafting onto organic particles already bonded to the NP surface (Supporting Information, Figure S3). As the sample is heated, the outer layers are removed, followed by the layer attached directly to the surface. In addition, the outer layer peak seems to shift to higher temperatures as the carbon chain gets longer. This shift to higher temperatures could be because of the formation of multiple layers and an increase in mass with the longer chains. A similar shift to higher temperature with corresponding increase in mass was seen in the TGA of gold NPs stabilized with thiols of increasing mass.[45] This multilayer formation by diazonium salt chemistry has been proposed in other literature that examines the attachment of organic molecules to gold NPs or surfaces.[46,47] A rough calculation using the TGA data and assuming that the NPs are spherical, gives ~15 groups/nm$^2$ on the surface of the NP. This seems to point to possible multilayer formation, but further studies are needed with transmission electron microscopy and other techniques.

The increasing hydrophobic nature of the organic modifiers led to the investigation of the hydrophobic properties of the resulting grafted NPs. This investigation was accomplished by


DOI: 10.1021/acs.langmuir.9b00201
Langmuir XXXX, XXX, XXX–XXX

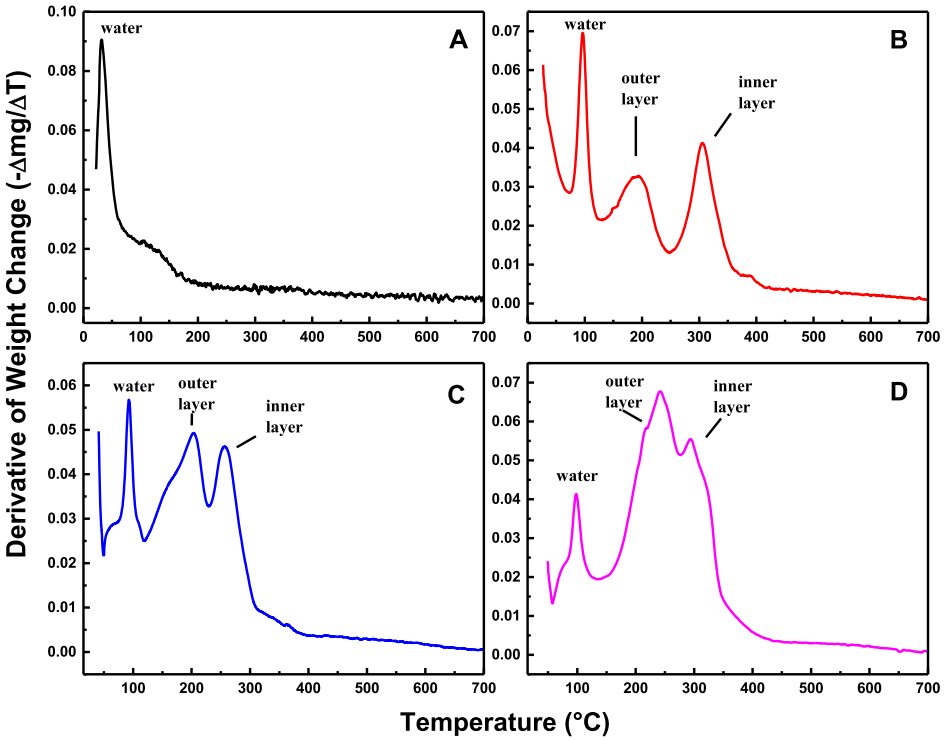



**Figure 6.** Weight loss derivative plots from TGA analysis for (A) unmodified $CeO_2$, (B) 4-methylbenzene-grafted $CeO_2$, (C) 4-ethylbenzene-grafted $CeO_2$, and (D) 4-*n*-butylbenzene-grafted $CeO_2$.

producing a pressed pellet of the NP specimens and then by performing a static water contact angle (SWCA) test. Materials that exhibit SWCAs below 90° are considered hydrophilic, while those above 90° are considered hydrophobic. If the water contact angle is above 150°, the material can be classified as superhydrophobic. Table 1 presents the water contact angles

**Table 1. Contact Angles for Pressed Pellets of Grafted NPs**

| NPs | contact angle ($n$ = 3) |
|---|---|
| bare $CeO_2$ | |
| 4-methylbenzene diazonium grafted | 33.6° ± 4.7° |
| 4-ethylbenzene diazonium grafted | 62.5° ± 6.5° |
| 4-*n*-butylbenzene diazonium grafted | 124.9° ± 6.9° |

for the grafted $CeO_2$ NPs. Cerium oxide by itself is slightly hydrophilic, and no water contact angles could be measured for the pellet of pure $CeO_2$ powder.

The increases in contact angles confirm that the particles become more hydrophobic as the carbon chain length is increased, as the 4-*n*-butyl-grafted NPs are well within the hydrophobic range. Additional modifications, such as using even longer carbon chains, may be able to enhance the hydrophobicity into the superhydrophobic range. A water droplet sitting upon a pressed pellet of the 4-*n*-butyl-grafted NPs (Figure 7) verifies that the hydrophobicity of $CeO_2$ can be changed through the use of organic modifiers. The formation of multilayers as suggested by the TGA results may be helping to increase the hydrophobicity of the NPs. While this multilayer formation was a desirable trait for controlling the hydrophobicity, it also has the potential to limit access to the $CeO_2$ surface. This limited access to the surface could introduce problems for certain applications that rely on cerium oxide's redox capabilities. However, the grafting process

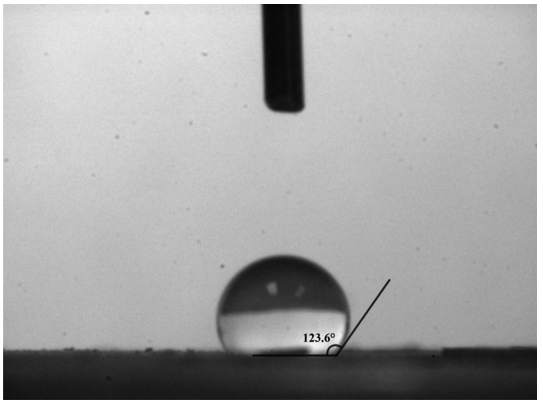



**Figure 7.** Image showing the water contact angle test on a pressed pellet of $CeO_2$ NPs grafted with 4-*n*-butylbenzene diazonium chloride. A contact angle of 123.6° was measured for this sample.

described in this work allows for a variety of R groups in surface modification of the cerium oxide NPs. Functionalizing the cerium oxide surface with a different group such as a carboxylic acid could enable the NPs to interact with metal ions in a solution or with a metal surface through an electrostatic interaction. Such an interaction would enable the cerium oxide NPs to be more compatible in an electrolytic solution for formation of coatings or a metal composite matrix.

## CONCLUSIONS

A facile method of functionalizing the surface of $CeO_2$ NPs in aqueous solution at room temperature was confirmed. The use of a chemical reducing agent as ascorbic acid is an effective means of grafting to NPs. The grafting mechanism of diazonium salts to $CeO_2$ NPs likely proceeds through terminal oxygens on the surface of the NPs. Grafting aryl diazonium


DOI: 10.1021/acs.langmuir.9b00201
Langmuir XXXX, XXX, XXX−XXX

salts to $CeO_2$ NPs does not affect the underlying crystal structure and should not inhibit catalytic function of the NP that relies on this crystal structure. The formation of multilayers is possible through the use of the diazonium salt grafting process. For some applications that depend on the redox abilities of $CeO_2$, further optimizations of the grafting procedure can be made. This work highlighted the control of physical properties for NPs such as hydrophobicity through the use of an easy-to-use grafting technique. Other physical/chemical properties may be enhanced by choice of the functional groups (such as fluoroalkyl groups) used in the grafting procedure. This research opens up potential new applications for NPs such as $CeO_2$ and extends the range of environments such as electrodeposition solutions in which they can be used. Possibly the NPs can be tailored to enhance the performance in catalytic reactions in which $CeO_2$ is important.

## ■ ASSOCIATED CONTENT

### Supporting Information

The Supporting Information is available free of charge on the ACS Publications website at DOI: 10.1021/acs.langmuir.9b00201.

Infrared spectra; $^{13}C$ NMR spectra; proposed sites for organic attachment; and formation of stable diazonium salts (PDF)

## ■ AUTHOR INFORMATION


### Corresponding Author

*E-mail: tgolden@unt.edu. Phone: 940-565-2888 (T.D.G.).

### ORCID

Teresa D. Golden: 0000-0003-4493-7228


### Notes

The authors declare no competing financial interest.

## ■ ACKNOWLEDGMENTS

The authors acknowledge the Advanced Materials and Manufacturing Processes Institute (AMMPI) as well as the University of North Texas Chemistry Department for financial support toward the completion of this study.

## ■ REFERENCES


(1) Steele, B. Mass transport in materials incorporated in electrochemical energy conversion systems. *Solid State Ionics* **1984**, *12*, 391−406.

(2) Mogensen, M.; Sammes, N. M.; Tempsett, G. A. Physical, chemical and electrochemical properties of pure and doped ceria. *Solid State Ionics* **2000**, *129*, 63−94.

(3) Tschöpe, A.; Schaadt, D.; Birringer, R.; Ying, J. Y. Catalytic properties of nanostructured metal oxides synthesized by inert gas condensation. *Nanostruct. Mater.* **1997**, *9*, 423−432.

(4) Tye, L.; El-Masry, N. A.; Chikyow, T.; McLarty, P.; Bedair, S. M. Electrical characteristics of epitaxial $CeO_2$ on Si(111). *Appl. Phys. Lett.* **1994**, *65*, 3081.

(5) Ishizaki, T.; Masuda, Y.; Sakamoto, M. Corrosion Resistance and Durability of superhydrophobic surface formed on magnesium alloy created with nanostructured cerium oxide film and fluoroalkylsilane molecules in corrosive NaCl aqueous solution. *Langmuir* **2011**, *27*, 4780−4788.

(6) Rivera, B. F.; Johnson, B. Y.; O'Keefe, M. J.; Fahrenholtz, W. G. Deposition and characterization of cerium oxide conversion coatings on aluminum alloy 7075-T6. *Surf. Coat. Technol.* **2004**, *176*, 349−356.

(7) Wang, A. Q.; Golden, T. D. Electrodeposition of oriented cerium oxide films. *Int. J. Electrochem.* **2013**, *2013*, 1−10.

(8) Qi, R.-J.; Zhu, Y.-J.; Cheng, G.-F.; Huang, Y.-H. Sonochemical synthesis of single-crystalline $CeOHCO_3$ rods and their thermal conversion to $CeO_2$ rods. *Nanotechnology* **2005**, *16*, 2502−2506.

(9) Natile, M. M.; Glisenti, A. Nanostructured Oxide-Based Powders:Investigation of the Growth Mode of the $CeO_2$ Clusters on the YSZ Surface. *J. Phys. Chem. B* **2006**, *110*, 2515−2521.

(10) Chen, H.-I.; Chang, H.-Y. Synthesis of nanocrystalline cerium oxide particles by the precipitation method. *Ceram. Int.* **2005**, *31*, 795−802.

(11) Feng, X.; Sayle, D. C.; Wang, Z. L.; Paras, M. S.; Santora, B.; Sutorik, A. C.; Sayle, T. X. T.; Yang, Y.; Ding, Y.; Wang, X.; Her, Y. Converting Ceria Polyhedral Nanoparticles into Single-Crystal Nanospheres. *Science* **2006**, *312*, 1504−1508.

(12) Li, L.; Chen, Y. Preparation of nanometer-scale $CeO_2$ particles via a complex thermo-decomposition method. *Mater. Sci. Eng., A* **2005**, *406*, 180−185.

(13) Darroudi, M.; Hakimi, M.; Sarani, M.; Kazemi Oskuee, R.; Khorsand Zak, A.; Gholami, L. Facile synthesis, characterization, and evaluation of neurotoxicity effect of cerium oxide nanoparticles. *Ceram. Int.* **2013**, *39*, 6917−6921.

(14) Yadav, T. P.; Srivastava, O. N. Synthesis of nanocrystalline cerium oxide by high energy ball milling. *Ceram. Int.* **2012**, *38*, 5783−5789.

(15) Wang, A. Q.; D'Souza, N.; Golden, T. D. Electrosynthesis of nanocrystalline cerium oxide/layered silicate powders. *J. Mater. Chem.* **2006**, *16*, 481−488.

(16) Zhou, Y.; Phillips, R. J.; Switzer, J. A. Electrochemical synthesis and sintering of nanocrystalline cerium (IV) oxide powders. *J. Am. Ceram. Soc.* **1995**, *78*, 981−985.

(17) Trovarelli, A.; Boaro, M.; Rocchini, E.; de Leitenburg, C.; Dolcetti, G. Some recent developments in the characterization of ceria-based catalysts. *J. Alloys Compd.* **2001**, *323*−*324*, 584−591.

(18) Zhang, F.; Chan, S.-W.; Spanier, J. E.; Apak, E.; Jin, Q.; Robinson, R. D.; Herman, I. P. Cerium oxide nanoparticles: size selective formation and structure analysis. *Appl. Phys. Lett.* **2002**, *80*, 127−129.

(19) Spanier, J. E.; Robinson, R. D.; Zhang, F.; Chan, S.-W.; Herman, I. P. Size-dependent properties of $CeO_2$-y nanoparticles as studied by Raman scattering. *Phys. Rev. B: Condens. Matter Mater. Phys.* **2001**, *64*, 245407−245415.

(20) Tsunekawa, S.; Sivamohan, R.; Ito, S.; Kasuya, A.; Fukuda, T. Structural study on monosize $CeO_{2-x}$ nano-particles. *Nanostruct. Mater.* **1999**, *11*, 141−147.

(21) McBride, J. R.; Hass, K. C.; Poindexter, B. D.; Weber, W. H. Raman and x-ray studies of $Ce_{1-x}RE_xO_{2-y}$ where RE = La, Pr, Nd, Eu, Gd, and Tb. *J. Appl. Phys.* **1994**, *76*, 2435−2441.

(22) Zhang, R.; Zhong, Q.; Zhao, W.; Yu, L.; Qu, H. Promotional effect of fluorine on the selective catalytic reduction of NO with $NH_3$ over $CeO_2$-$TiO_2$ catalyst at low temperature. *Appl. Surf. Sci.* **2014**, *289*, 237−244.

(23) Qi, G.; Yang, R. T.; Chang, R. $MnO_x$-$CeO_2$ mixed oxides prepared by co-precipitation for selective catalytic reduction of NO with $NH_3$ at low temperatures. *Appl. Catal., B* **2004**, *51*, 93−106.

(24) Galli, C. Radical reactions of arenediazonium ions: An easy entry into the chemistry of the aryl radical. *Chem. Rev.* **1988**, *88*, 765−792.

(25) Delamar, M.; Hitmi, R.; Pinson, J.; Saveant, J. M. Covalent modification of carbon surfaces by grafting of functionalized aryl radicals produced from electrochemical reduction of diazonium salts. *J. Am. Chem. Soc.* **1992**, *114*, 5883−5884.

(26) Allongue, P.; Delamar, M.; Desbat, B.; Fagebaume, O.; Hitmi, R.; Pinson, J.; Savéant, J.-M. Covalent Modification of Carbon Surfaces by Aryl Radicals Generated from the Electrochemical Reduction of Diazonium Salts. *J. Am. Chem. Soc.* **1997**, *119*, 201−207.

(27) Adenier, A.; Cabet-Deliry, E.; Chaussé, A.; Griveau, S.; Mercier, F.; Pinson, J.; Vautrin-Ul, C. Grafting of Nitrophenyl Groups on Carbon and Metallic Surfaces without Electrochemical Induction. *Chem. Mater.* **2005**, *17*, 491−501.




DOI: 10.1021/acs.langmuir.9b00201
*Langmuir* XXXX, XXX, XXX−XXX

(28) Kosynkin, D.; Bockman, T. M.; Kochi, J. K. Thermal (Iodide) and Photoinduced Electron-Transfer Catalysis in Biaryl Synthesis via Aromatic Arylations with Diazonium Salts. *J. Am. Chem. Soc.* **1997**, *119*, 4846−4855.
(29) Mooste, M.; Kibena-Põldsepp, E.; Marandi, M.; Matisen, L.; Sammelselg, V.; Podvorica, F. I.; Tammeveski, K. Surface and electrochemical characterization of aryl films grafted on polycrystalline copper from the diazonium compounds using the rotating disk electrode method. *J. Electroanal. Chem.* **2018**, *817*, 89−100.
(30) Chamoulaud, G.; Bélanger, D. Spontaneous Derivatization of a Copper Electrode with in Situ Generated Diazonium Cations in Aprotic and Aqueous Media. *J. Phys. Chem. C* **2007**, *111*, 7501−7507.
(31) Berger, F.; Delhalle, J.; Mekhalif, Z. Hybrid coating on steel: ZnNi electrodeposition and surface modification with organothiols and diazonium salts. *Electrochim. Acta* **2008**, *53*, 2852−2861.
(32) Adenier, A.; Bernard, M.-C.; Chehimi, M. M.; Cabet-Deliry, E.; Desbat, B.; Fagebaume, O.; Pinson, J.; Podvorica, F. Covalent Modification of Iron Surfaces by Electrochemical Reduction of Aryldiazonium Salts. *J. Am. Chem. Soc.* **2001**, *123*, 4541−4549.
(33) Lehr, J.; Williamson, B. E.; Flavel, B. S.; Downard, A. J. Reaction of Gold Substrates with Diazonium Salts in Acidic Solution at Open-Circuit Potential. *Langmuir* **2009**, *25*, 13503−13509.
(34) Liang, H.; Tian, H.; McCreery, R. L. Normal and surface-enhanced Raman spectroscopy of nitroazobenzene submonolayers and multilayers on carbon and silver surfaces. *Appl. Spectrosc.* **2007**, *61*, 613−620.
(35) Chhin, D.; Polcari, D.; Bodart-Le Guen, C.; Tomasello, G.; Cicoira, F.; Schougaard, S. B. Diazonium-Based Anchoring of PEDOT on Pt/Ir Electrodes via Diazonium Chemistry. *J. Electrochem. Soc.* **2018**, *165*, G3066−G3070.
(36) Wang, D.; Buriak, J. M. Trapping Silicon Surface-Based Radicals. *Langmuir* **2006**, *22*, 6214−6221.
(37) Merson, A.; Dittrich, T.; Zidon, Y.; Rappich, J.; Shapira, Y. Charge transfer from $TiO_2$ into adsorbed benzene diazonium compounds. *Appl. Phys. Lett.* **2004**, *85*, 1075−1076.
(38) Bell, K. J.; Brooksby, P. A.; Polson, M. I. J.; Downard, A. J. Evidence for covalent bonding of aryl groups to $MnO_2$ nanorods from diazonium-based grafting. *Chem. Commun.* **2014**, *50*, 13687−13690.
(39) Yang, S.; Pan, Q.; Liu, J. Improving the cycleability of Si anodes by covalently grafting with 4-carboxyphenyl groups. *Electrochem. Commun.* **2010**, *12*, 479−482.
(40) Griffete, N.; Herbst, F.; Pinson, J.; Ammar, S.; Mangeney, C. Preparation of Water-Soluble Magnetic Nanocrystals Using Aryl Diazonium Salt Chemistry. *J. Am. Chem. Soc.* **2011**, *133*, 1646−1649.
(41) Kumar, V. K. R.; Gopidas, K. R. Synthesis and characterization of gold-nanoparticle-cored dendrimers stabilized by metal-carbon bonds. *Chem.—Asian J.* **2010**, *5*, 887−896.
(42) Clancy, A. J.; Serginson, J. M.; Greenfield, J. L.; Shaffer, M. S. P. Systemic comparison of single-walled carbon nanotube/poly(vinyl acetate) graft-to reactions. *Polymer* **2017**, *133*, 263−271.
(43) Sheng, M.; Frurip, D.; Gorman, D. Reactive chemical hazards of diazonium salts. *J. Loss Prev. Process Ind.* **2015**, *38*, 114−118.
(44) Furness, B. S.; Hannaford, A. J.; Smith, P. W. G.; Tatchell, A. R. *Vogel's Textbook of Practical Organic Chemistry*; Longman Scientific & Technical: Essex, U.K., 1989; pp 920−922.
(45) Isaacs, S. R.; Choo, H.; Ko, W.-B.; Shon, Y.-S. Chemical, thermal, and ultrasonic Stability of hybrid nanoparticles and nanoparticle multilayer films. *Chem. Mater.* **2006**, *18*, 107−114.
(46) Laurentius, L.; Stoyanov, S. R.; Gusarov, S.; Kovalenko, A.; Du, R.; Lopinski, G. P.; McDermott, M. T. Diazonium-Derived aryl films on gold nanoparticles: Evidence for a carbon-gold covalent bond. *ACS Nano* **2011**, *5*, 4219−4227.
(47) Shewchuk, D. M.; McDermott, M. T. Comparison of diazonium salt derived and thiol derived nitrobenzene layers on gold. *Langmuir* **2009**, *25*, 4556−4563.


DOI: 10.1021/acs.langmuir.9b00201
*Langmuir* XXXX, XXX, XXX−XXX